

BOUNDARY ELEMENT METHOD IN DYNAMIC CRACK ANALYSIS

PIOTR FEDELIŃSKI

Department of Strength of Materials and Computational Mechanics

Silesian Technical University of Gliwice

e-mail: fedel@rmt4.kmt.polsl.gliwice.pl

The boundary element method applications to dynamic fracture mechanics are presented. In the present approach displacement and traction boundary integral equations are used for crack representation. The time-dependent solutions are obtained using the time domain method, integral transform method or dual reciprocity method. The dynamic stress intensity factors are calculated using crack opening displacements and the path-independent \hat{J} -integral. Some new applications of these methods are also shown.

Key words: the boundary element method, dynamic fracture mechanics

1. Introduction

Dynamic fracture mechanics deals with analysis of the growth, arrest and branching of moving cracks in structures subjected to dynamic loads (Freund, 1990; Neimitz, 1994). The structures with arbitrary shape and time-dependent boundary conditions need to be analyzed using numerical methods. The boundary element method (BEM) has been successfully applied to stationary and growing cracks in infinite and finite domains in elastostatics (Cruse, 1988; Aliabadi and Rooke, 1991) and elastodynamics (Dominguez, 1993). The application of BEM in fracture mechanics is particularly attractive, because it allows for accurate determination of the stress field, and because a remeshing, which is required for propagating cracks is much simpler than in the domain numerical methods.

Solution to a general crack problem cannot be achieved in a single-region analysis by a direct application of BEM, because the coincidence of crack nodes gives rise to a singular system of algebraic equations. The boundary integral

equations for two coincident points on both surfaces of the crack are identical, because they have the same coordinates, and integrals are calculated along the same boundary. Several formulations have been developed to overcome this difficulty.

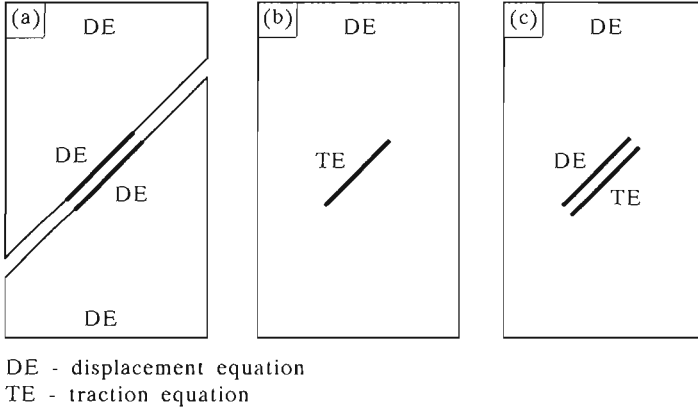


Fig. 1. Crack modelling methods using BEM: (a) subregion method, (b) displacement discontinuity method, (c) dual method

In *the subregion method* the structure is divided into subdomains along a continuation of crack surfaces (see Fig.1a); these subregions are assembled using the equilibrium and compatibility conditions along the new internal boundary. The displacement boundary integral equation is used for all nodes.

Another method is *the displacement discontinuity method*. In this method only one of the crack surfaces is discretized (see Fig.1b). The displacement boundary integral equation is used for nodes on the external boundary and the traction equation for nodes on the crack surface. These equations are expressed in relative displacements of the crack surfaces.

A non-singular system of equations can be obtained by using two different boundary integral equations for coincident points, for example the displacement and traction equations (see Fig.1c). The displacement equation is used for the remaining nodes. The unknown absolute values of displacements and tractions along the crack surfaces and other boundaries of the body are obtained directly by solving of the system of equations.

The last method, called *the dual boundary element method* (DBEM) was developed by Portela et al. (1992), (1993) for stationary and growing cracks in 2D analysis. This method was extended by Mi and Aliabadi (1992), (1994) onto stationary and growing cracks in 3D analysis. The dynamic solutions are usually obtained by three different formulations; i.e., time domain method,

integral transform method and dual reciprocity method (Dominguez, 1993; Burczyński, 1995). The details of numerical implementation of these methods in dynamic fracture mechanics were presented in several papers. Fedeliński et al. presented applications of the DBEM combined with the dual reciprocity method (1993a,b,c), (1994a), the time domain method (1994b,c), (1995a) and the integral transform methods (1996a) and Fedeliński (1996) for stationary cracks in structures subjected to dynamic loading. The accuracy and efficiency of these methods were compared by Fedeliński et al. (1995b), (1996b) and Fedeliński (1997a,c). The application of time-domain method to dynamic analysis of growing cracks was shown by Fedeliński et al. (1997) and Fedeliński (1997b). The methods were extended to three-dimensional dynamic crack problems by Wen, Aliabadi and Rooke (1997a,b) and Fedeliński (1998a,b,c).

In this paper the DBEM and the three approaches: time-domain, integral transform and dual reciprocity method, respectively, are presented. For each method the displacement and the traction boundary integral equations for cracks are formulated. The forms of the final matrix, which are suitable for the numerical application are given. The dynamic stress intensity factors are calculated using both the crack opening displacements and the path independent \hat{J} -integral. Some new applications of these methods are also shown.

2. Time domain method

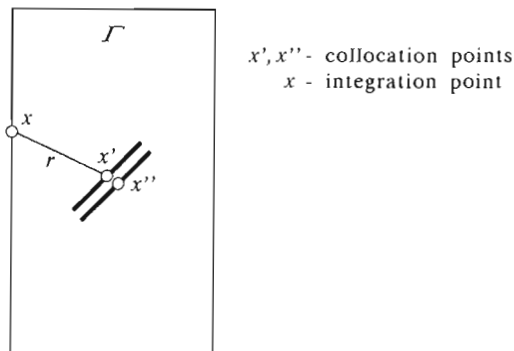


Fig. 2. Collocation points on crack surfaces

Consider a homogeneous and isotropic linear elastic body limited by a boundary Γ . For the body which is not subjected to the body forces and

which has zero initial displacements and velocities, the displacements of points \mathbf{x}' and \mathbf{x}'' on the smooth crack surfaces, shown in Fig.2, can be represented by the following boundary integral equation

$$\begin{aligned} \frac{1}{2}u_i(\mathbf{x}', t) + \frac{1}{2}u_i(\mathbf{x}'', t) = & \int_0^t \left[\int_{\Gamma} U_{ij}(\mathbf{x}', t; \mathbf{x}, \tau) t_j(\mathbf{x}, \tau) d\Gamma(\mathbf{x}) \right] d\tau + \\ & - \int_0^t \left[\oint_{\Gamma} T_{ij}(\mathbf{x}', t; \mathbf{x}, \tau) u_j(\mathbf{x}, \tau) d\Gamma(\mathbf{x}) \right] d\tau \end{aligned} \quad (2.1)$$

where

$U_{ij}(\mathbf{x}', t; \mathbf{x}, \tau), T_{ij}(\mathbf{x}', t; \mathbf{x}, \tau)$ – fundamental solutions of elastodynamics

$u_j(\mathbf{x}, \tau), t_j(\mathbf{x}, \tau)$ – displacements and tractions, respectively, at the boundary

\mathbf{x} – boundary point

t – time of observation

\oint – Cauchy principal value integral.

The summation convention is used for the repeated subscripts.

The traction integral equation is obtained by differentiating the displacement equation, applying Hooke's law and multiplying by the outward normal at the collocation point. For the points which belong to the smooth crack surfaces the traction equation is

$$\begin{aligned} \frac{1}{2}t_j(\mathbf{x}', t) - \frac{1}{2}t_j(\mathbf{x}'', t) = & n_i(\mathbf{x}') \left\{ \int_0^t \left[\int_{\Gamma} U_{kij}(\mathbf{x}', t; \mathbf{x}, \tau) t_k(\mathbf{x}, \tau) d\Gamma(\mathbf{x}) \right] d\tau + \right. \\ & \left. - \int_0^t \left[\oint_{\Gamma} T_{kij}(\mathbf{x}', t; \mathbf{x}, \tau) u_k(\mathbf{x}, \tau) d\Gamma(\mathbf{x}) \right] d\tau \right\} \end{aligned} \quad (2.2)$$

where

$U_{kij}(\mathbf{x}', t; \mathbf{x}, \tau), T_{kij}(\mathbf{x}', t; \mathbf{x}, \tau)$ – other fundamental solutions of elastodynamics

$n_i(\mathbf{x}')$ – components of the outward normal at the collocation point \mathbf{x}'

\oint – Hadamard principal value integral.

The numerical solution to a general mixed-mode crack problem is obtained after discretizing both space and time variations. The boundary Γ of the body

is divided into boundary elements. The observation time t is divided into time steps. The displacements and tractions are approximated within each element using space interpolation functions, and within each time step using temporal interpolation functions. The boundary integral equations are applied to all nodes of the boundary elements. A distinct set of boundary integral equations is obtained by applying the displacement equation to collocation points along the external boundary and along one of the crack faces, and the traction equation to collocation points on the opposite surface of the crack.

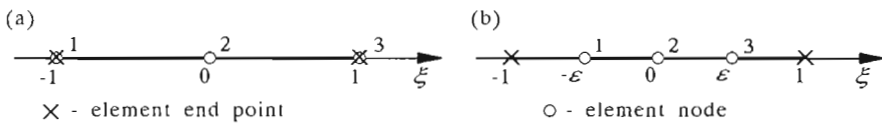


Fig. 3. Quadratic boundary elements for 2D problems: (a) continuous element, (b) discontinuous element

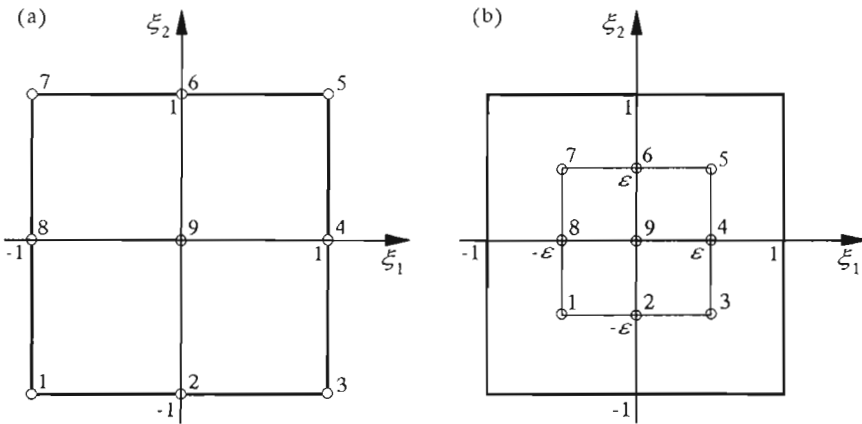


Fig. 4. Quadratic boundary elements for 3D problems: (a) continuous element, (b) discontinuous element

Quadratic elements are used for the discretization of the boundary. The displacements and tractions are interpolated using continuous elements for the external boundary and discontinuous elements on the crack faces. The geometry is approximated by using continuous quadratic elements. The continuous and discontinuous quadratic boundary elements used for 2D and 3D problems are shown in Fig.3 and Fig.4, respectively. The elements are shown in the local coordinate system, where the parameter $\epsilon < 1$. The displacements are

approximated within each time step by using linear interpolating functions and the tractions are piecewise constant.

The time integrals with simple temporal shape functions can be calculated analytically. The set of discretized boundary equations can be written in a matrix form at the time step N as

$$\tilde{\mathbf{H}}^{NN} \mathbf{u}^N = \tilde{\mathbf{G}}^{NN} \mathbf{t}^N + \sum_{n=1}^{N-1} (\tilde{\mathbf{G}}^{Nn} \mathbf{t}^n - \tilde{\mathbf{H}}^{Nn} \mathbf{u}^n) \quad (2.3)$$

where \mathbf{u}^n , \mathbf{t}^n contain the nodal values of displacements and tractions at the time step n ; $\tilde{\mathbf{H}}^{Nn}$ and $\tilde{\mathbf{G}}^{Nn}$ depend on the integrals of the fundamental solutions and interpolating functions. The superscripts Nn emphasize that the matrix depends on the difference between the time steps N and n . The columns of matrices $\tilde{\mathbf{H}}^{Nn}$, $\tilde{\mathbf{G}}^{Nn}$ are reordered according to the boundary conditions, yielding new matrices $\tilde{\mathbf{A}}^{NN}$ and $\tilde{\mathbf{B}}^{NN}$. The matrix $\tilde{\mathbf{A}}^{NN}$ is multiplied by the vector \mathbf{x}^N of unknown displacements and tractions and the matrix $\tilde{\mathbf{B}}^{NN}$ by the vector \mathbf{y}^N of known boundary conditions as follows

$$\tilde{\mathbf{A}}^{NN} \mathbf{x}^N = \tilde{\mathbf{B}}^{NN} \mathbf{y}^N + \sum_{n=1}^{N-1} (\tilde{\mathbf{G}}^{Nn} \mathbf{t}^n - \tilde{\mathbf{H}}^{Nn} \mathbf{u}^n) \quad (2.4)$$

At each time step only the matrices, which correspond to the maximum difference $N - n$ are computed. The remaining matrices are known from previous steps. The matrices $\tilde{\mathbf{A}}^{NN}$ and $\tilde{\mathbf{B}}^{NN}$ are calculated in the first step only since they are the same at each time step; $\tilde{\mathbf{A}}^{Nn} = \tilde{\mathbf{A}}$ and $\tilde{\mathbf{B}}^{Nn} = \tilde{\mathbf{B}}$. Eq (2.4) can be rewritten in a simpler form as

$$\tilde{\mathbf{A}} \mathbf{x}^N = \tilde{\mathbf{f}}^N \quad (2.5)$$

where

$$\tilde{\mathbf{f}}^N = \tilde{\mathbf{B}} \mathbf{y}^N + \sum_{n=1}^{N-1} (\tilde{\mathbf{G}}^{Nn} \mathbf{t}^n - \tilde{\mathbf{H}}^{Nn} \mathbf{u}^n) \quad (2.6)$$

is a known vector. The matrix equation is solved step-by-step giving the unknown displacements and tractions at each time step.

3. Integral transform method

Accepting the same assumptions as for the time domain method, the integral transform of the displacements of points \mathbf{x}' and \mathbf{x}'' which belong to

smooth crack surfaces can be obtained from the following boundary integral equation

$$\begin{aligned} \frac{1}{2}\bar{u}_i(\mathbf{x}', s) + \frac{1}{2}\bar{u}_i(\mathbf{x}'', s) &= \int_{\Gamma} \bar{U}_{ij}(\mathbf{x}', \mathbf{x}, s)\bar{t}_j(\mathbf{x}, s) d\Gamma(\mathbf{x}) + \\ &- \int_{\Gamma} \bar{T}_{ij}(\mathbf{x}', \mathbf{x}, s)\bar{u}_j(\mathbf{x}, s) d\Gamma(\mathbf{x}) \end{aligned} \tag{3.1}$$

where

- $\bar{U}_{ij}(\mathbf{x}', \mathbf{x}, s), \bar{T}_{ij}(\mathbf{x}', \mathbf{x}, s)$ – integral transforms of fundamental solutions of elastodynamics
- $\bar{u}_j(\mathbf{x}, s), \bar{t}_j(\mathbf{x}, s)$ – integral transforms of the displacements and tractions respectively, at the boundary

s – integral transform parameter.

General forms of the boundary integral equations and transformed fundamental solutions of elastodynamics are the same for the Laplace and Fourier transform methods.

The integral transform of the traction equation for the points which belong to smooth crack surfaces is

$$\begin{aligned} \frac{1}{2}\bar{t}_j(\mathbf{x}', s) - \frac{1}{2}\bar{t}_j(\mathbf{x}'', s) &= n_i(\mathbf{x}') \left[\int_{\Gamma} \bar{U}_{kij}(\mathbf{x}', \mathbf{x}, s)\bar{t}_k(\mathbf{x}, s) d\Gamma(\mathbf{x}) + \right. \\ &- \left. \int_{\Gamma} \bar{T}_{kij}(\mathbf{x}', \mathbf{x}, s)\bar{u}_k(\mathbf{x}, s) d\Gamma(\mathbf{x}) \right] \end{aligned} \tag{3.2}$$

where $\bar{U}_{kij}(\mathbf{x}', \mathbf{x}, s)$ and $\bar{T}_{kij}(\mathbf{x}', \mathbf{x}, s)$ are the integral transforms of other fundamental solutions of elastodynamics.

In order to solve a general mixed-mode crack problem the boundary is discretized in the same way as for the time domain method. The boundary equations are applied to the boundary nodes. The set of discretized boundary integral equations can be written in a matrix form as

$$\bar{\mathbf{H}}\bar{\mathbf{u}} = \bar{\mathbf{G}}\bar{\mathbf{t}} \tag{3.3}$$

where $\bar{\mathbf{u}}$ and $\bar{\mathbf{t}}$ contain nodal values of the transformed displacements and tractions respectively, and $\bar{\mathbf{H}}$ and $\bar{\mathbf{G}}$ depend on integrals of the transformed fundamental solutions and the interpolating functions. The matrices $\bar{\mathbf{H}}$ and

$\bar{\mathbf{G}}$ are reordered according to the boundary conditions, in the same way as in elastostatics, to give new matrices $\bar{\mathbf{A}}$ and $\bar{\mathbf{B}}$. The matrix $\bar{\mathbf{A}}$ is multiplied by the vector $\bar{\mathbf{x}}$ of unknown transformed displacements and tractions and $\bar{\mathbf{B}}$ by the vector $\bar{\mathbf{y}}$ of known transformed boundary conditions, as follows

$$\bar{\mathbf{A}}\bar{\mathbf{x}} = \bar{\mathbf{B}}\bar{\mathbf{y}} \quad (3.4)$$

or

$$\bar{\mathbf{A}}\bar{\mathbf{x}} = \bar{\mathbf{f}} \quad (3.5)$$

where $\bar{\mathbf{f}} = \bar{\mathbf{B}}\bar{\mathbf{y}}$ is a known vector.

Eq (3.5) is solved giving the unknown transformed displacements and tractions for a particular integral transform parameter. For simple time variations of the prescribed boundary conditions their integral transforms can be calculated analytically. In order to obtain the unknown displacements and tractions as functions of time, the unknown transformed variables must be computed for a series of parameters. The final time-dependent solution can be obtained from a numerical inversion.

4. Dual reciprocity method

In this method the equations of motion are expressed in a boundary integral form using the fundamental solutions of elastostatics. This can be achieved by approximating the acceleration of a point \mathbf{x} of the body by a sum of N coordinate functions $f^n(\mathbf{x}^*, \mathbf{x})$ multiplied by unknown time-dependent coefficients $\ddot{\alpha}_l^n(\tau)$

$$\ddot{u}_l(\mathbf{x}, \tau) = \sum_{n=1}^N \ddot{\alpha}_l^n(\tau) f^n(\mathbf{x}^*, \mathbf{x}) \quad (4.1)$$

where the dot above the variable denotes the derivative with respect to time. The approximation function $f^n(\mathbf{x}^*, \mathbf{x}) = c + r(\mathbf{x}^*, \mathbf{x})$ is chosen, where c is a constant and $r(\mathbf{x}^*, \mathbf{x})$ is the distance between a defining point \mathbf{x}^* and the point \mathbf{x} . The defining point can be a boundary or domain point.

Using this assumption the displacement boundary equation of motion for the points which belong to the crack in a homogeneous and isotropic linear elastic body can be written as

$$\begin{aligned}
& \frac{1}{2}u_i(\mathbf{x}', \tau) + \frac{1}{2}u_i(\mathbf{x}'', \tau) - \int_{\Gamma} U_{ij}(\mathbf{x}', \mathbf{x})t_j(\mathbf{x}, \tau) d\Gamma(\mathbf{x}) + \\
& + \int_{\Gamma} T_{ij}(\mathbf{x}', \mathbf{x})u_j(\mathbf{x}, \tau) d\Gamma(\mathbf{x}) = \sum_{n=1}^N \rho \ddot{\alpha}_l^n(\tau) \left[\frac{1}{2}\hat{u}_l^n(\mathbf{x}^*, \mathbf{x}') + \frac{1}{2}\hat{u}_l^n(\mathbf{x}^*, \mathbf{x}'') + \right. \\
& \left. - \int_{\Gamma} U_{ij}(\mathbf{x}', \mathbf{x})\hat{t}_{lj}^n(\mathbf{x}^*, \mathbf{x}) d\Gamma(\mathbf{x}) + \int_{\Gamma} T_{ij}(\mathbf{x}', \mathbf{x})\hat{u}_{lj}^n(\mathbf{x}^*, \mathbf{x}) d\Gamma(\mathbf{x}) \right]
\end{aligned} \tag{4.2}$$

The traction integral equation for the points which belong to smooth crack surfaces, has the form

$$\begin{aligned}
& \frac{1}{2}t_j(\mathbf{x}', \tau) - \frac{1}{2}t_j(\mathbf{x}'', \tau) - n_i(\mathbf{x}') \left[\int_{\Gamma} U_{kij}(\mathbf{x}', \mathbf{x})t_k(\mathbf{x}, \tau) d\Gamma(\mathbf{x}) + \right. \\
& \left. - \int_{\Gamma} T_{kij}(\mathbf{x}', \mathbf{x})u_k(\mathbf{x}, \tau) d\Gamma(\mathbf{x}) \right] = \sum_{n=1}^N \rho \ddot{\alpha}_l^n(\tau) \left\{ \frac{1}{2}\hat{t}_{lj}^n(\mathbf{x}^*, \mathbf{x}') - \frac{1}{2}\hat{t}_{lj}^n(\mathbf{x}^*, \mathbf{x}'') + \right. \\
& \left. - n_i(\mathbf{x}') \left[\int_{\Gamma} U_{kij}(\mathbf{x}', \mathbf{x})\hat{t}_{lk}(\mathbf{x}^*, \mathbf{x}) d\Gamma(\mathbf{x}) - \int_{\Gamma} T_{kij}(\mathbf{x}', \mathbf{x})\hat{u}_{lk}(\mathbf{x}^*, \mathbf{x}) d\Gamma(\mathbf{x}) \right] \right\}
\end{aligned} \tag{4.3}$$

where ρ is the mass density; $U_{ij}(\mathbf{x}', \mathbf{x})$, $T_{ij}(\mathbf{x}', \mathbf{x})$, $U_{kij}(\mathbf{x}', \mathbf{x})$ and $T_{kij}(\mathbf{x}', \mathbf{x})$ are fundamental solutions of elastostatics; $\hat{u}_{lj}^n(\mathbf{x}^*, \mathbf{x})$ and $\hat{t}_{lj}^n(\mathbf{x}^*, \mathbf{x})$ are particular displacements and tractions, which correspond to the function $f^n(\mathbf{x}^*, \mathbf{x})$.

The boundary of the body is discretized as in the previous approaches. The displacements and the tractions, $u_j(\mathbf{x}, \tau)$, $t_j(\mathbf{x}, \tau)$ and $\hat{u}_{lj}^n(\mathbf{x}^*, \mathbf{x})$, $\hat{t}_{lj}^n(\mathbf{x}^*, \mathbf{x})$ within each element are approximated using the same interpolation functions. The boundary equations are formulated for the boundary nodes as in the other approaches. The displacement equations are formulated for the domain points, when they are used to improve the approximation of accelerations. The set of equations can be written in a matrix form as

$$\mathbf{H}\mathbf{u} - \mathbf{G}\mathbf{t} - \rho(\mathbf{H}\hat{\mathbf{u}} - \mathbf{G}\hat{\mathbf{t}})\ddot{\boldsymbol{\alpha}} = \mathbf{0} \tag{4.4}$$

where \mathbf{H} and \mathbf{G} depend on integrals of fundamental solutions and interpolating functions; they are the same as in elastostatics. The vectors \mathbf{u} , \mathbf{t} , $\hat{\mathbf{u}}$ and $\hat{\mathbf{t}}$ contain nodal values of the real and particular displacements and tractions. The relationship between $\ddot{\mathbf{u}}$ and $\ddot{\boldsymbol{\alpha}}$ is established by using Eq (4.1) at every

boundary and domain node. The resulting set of equations can be written in a matrix form

$$\ddot{\mathbf{u}} = \mathbf{F}\ddot{\boldsymbol{\alpha}} \quad (4.5)$$

where the entries of matrix \mathbf{F} are the values of function $f^n(\mathbf{x}^*, \mathbf{x})$ at all N nodes. The unknown coefficients $\ddot{\boldsymbol{\alpha}}$ can be expressed in terms of the accelerations $\ddot{\mathbf{u}}$ as follows

$$\ddot{\boldsymbol{\alpha}} = \mathbf{E}\ddot{\mathbf{u}} \quad (4.6)$$

Substitution of Eq (4.6) into Eq (4.4) gives

$$\mathbf{H}\mathbf{u} - \mathbf{G}\mathbf{t} - \rho(\mathbf{H}\hat{\mathbf{u}} - \mathbf{G}\hat{\mathbf{t}})\mathbf{E}\ddot{\mathbf{u}} = \mathbf{0} \quad (4.7)$$

or

$$\mathbf{H}\mathbf{u} - \mathbf{G}\mathbf{t} + \mathbf{M}\ddot{\mathbf{u}} = \mathbf{0} \quad (4.8)$$

where $\mathbf{M} = -\rho(\mathbf{H}\hat{\mathbf{u}} - \mathbf{G}\hat{\mathbf{t}})\mathbf{E}$ is the mass matrix of the structure. The system of equations of motion (4.8) is modified, according to the boundary conditions, and can be solved using a direct integration method.

5. Dynamic stress intensity factors

One of the most important parameters in dynamic fracture mechanics is the dynamic stress intensity factor (DSIF), since it characterizes the stress field in the vicinity of crack, and controls the crack growth. In the present approach it is determined from the crack opening displacements and the path independent $\hat{\mathcal{J}}$ -integral.

In the first method, the DSIFs are calculated by comparing the numerical values of crack surfaces displacements with the known analytical form of the expression for the displacement field at the crack tip. The DSIFs obtained from the crack opening displacements (COD) are

$$K_I = \frac{2\mu}{\kappa + 1} \sqrt{\frac{\pi}{2r}} \Delta u_2 \quad \text{and} \quad K_{II} = \frac{2\mu}{\kappa + 1} \sqrt{\frac{\pi}{2r}} \Delta u_1 \quad (5.1)$$

where

- μ – shear modulus
- $\Delta u_1, \Delta u_2$ – relative displacements in the tangential and perpendicular directions, respectively, of the corresponding points on opposite crack faces
- r – distance of these points from the crack tip
- ν – Poisson ratio

and $\kappa = 3 - 4\nu$ for plane strain and $\kappa = (3 - \nu)/(1 + \nu)$ for plane stress.

In the second method, the DSIFs are calculated from the path independent \hat{J} -integral

$$\hat{J}^\beta = \int_{S+S_c} (W^\beta n_1 - t_i^\beta u_{i,1}^\beta) dS + \int_A \rho \ddot{u}_i^\beta u_{i,1}^\beta dA \quad \beta = I, II \quad (5.2)$$

where

- S - arbitrary curve surrounding the crack tip
- S_c - crack surfaces
- A - area enclosed by S and S_c
- W - strain energy density
- n_1 - component of the unit outward normal to the boundary of A

and a subscript preceded by a comma denotes differentiation with respect to that coordinate, the superscripts β denote the deformation modes I or II .

Displacements, derivatives of displacements, strain, stresses, tractions and accelerations are calculated using the appropriate boundary integral equations and they are decomposed into components for the symmetric mode I and antisymmetric mode II .

Knowing the \hat{J}^β -integral we can calculate the stress intensity factors, as follows

$$K_I = \sqrt{\frac{8\mu}{\kappa + 1} \hat{J}^I} \quad \text{and} \quad K_{II} = \sqrt{\frac{8\mu}{\kappa + 1} \hat{J}^{II}} \quad (5.3)$$

The sign of K_I and K_{II} is determined by the relative displacements of the crack surfaces.

6. Numerical examples

In this section three different numerical examples are shown to demonstrate the application of the methods. First example, a crank with two edge cracks presents the application of the time-domain and Laplace transform methods. The second example, a rotating disc with two edge cracks shows the application of the dual reciprocity method for a structure subjected to the body forces. The third example, a rectangular bar with an internal square crack, shows the application of the Laplace and Fourier transform methods to 3D problems. The DSIFs are obtained from COD calculations for the time domain and the integral transform methods; and from the \hat{J} -integral for the dual reciprocity

method. The structures are instantaneously loaded by a stress σ_0 at the time $\tau = 0$. The DSIFs are normalized with respect to

$$K_0 = \sigma_0 \sqrt{\pi a} \tag{6.1}$$

where a defines the crack length. Dynamic loading and the normalizing factor for the second examples are defined in the subsection. The material properties are: Young modulus $E = 0.2 \cdot 10^{12}$ Pa; Poisson ratio $\nu = 0.3$; mass density $\rho = 8000 \text{ kg m}^{-3}$. In the third example, the Poisson ratio is $\nu = 0.2$. The plane strain is assumed for two-dimensional problems.

6.1. Crank with two edge cracks

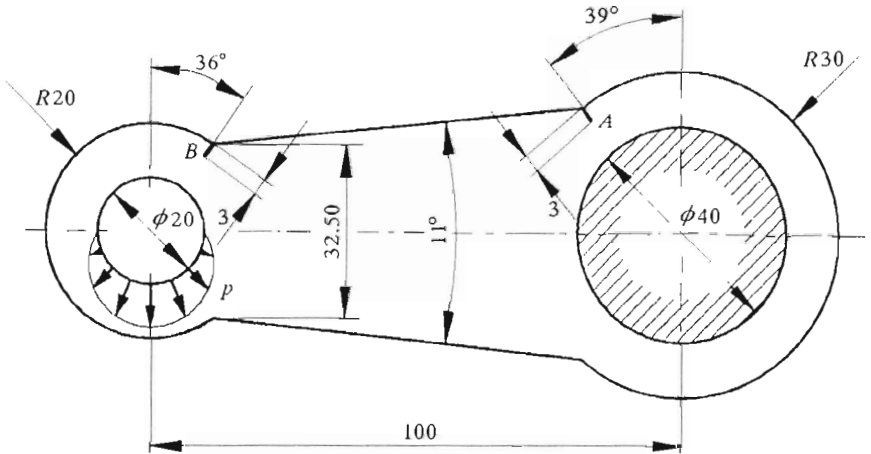


Fig. 5. Crank with two edge cracks

A crank with two holes contains two edge cracks. The dimensions of the crank, expressed in millimeters, are shown in Fig.5. One hole is constrained and the second is loaded by a suddenly applied normal pressure with a sine distribution. The boundary is divided into 68 quadratic elements. The solutions are obtained by using 50 parameters for the Laplace transform method and the time steps $\Delta\tau = 3\mu\text{s}$ for the time domain method. The normalized dynamic stress intensity factors versus time for both crack tips are shown in Fig.6. It can be seen that the solutions obtained by both methods are similar.

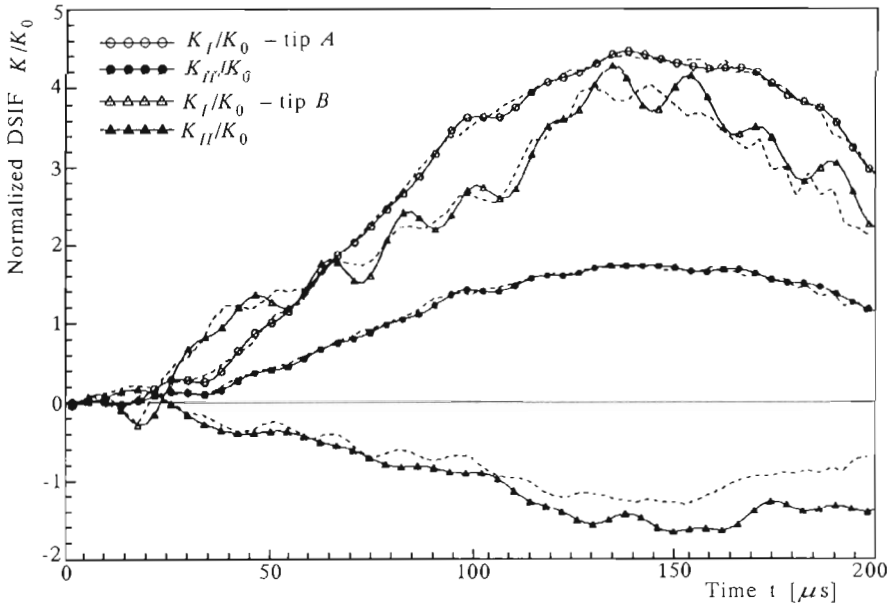


Fig. 6. Normalized DSIFs versus time for the crank with two edge cracks (Laplace transform method - solid line, time domain method - dashed line)

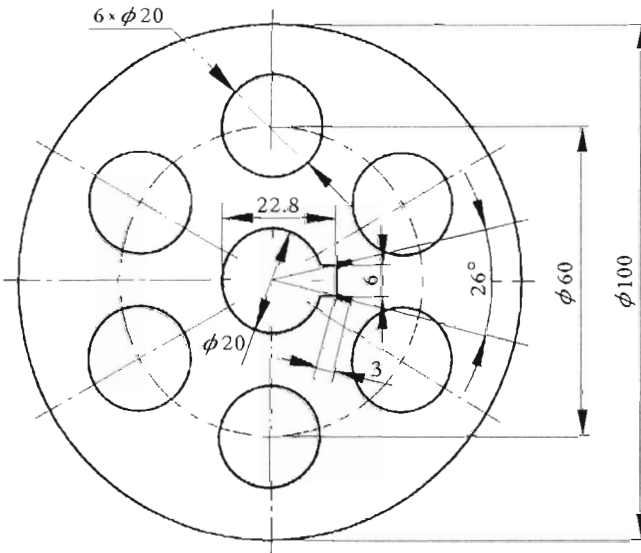


Fig. 7. Rotating disc with two edge cracks

6.2. Rotating disc with two edge cracks

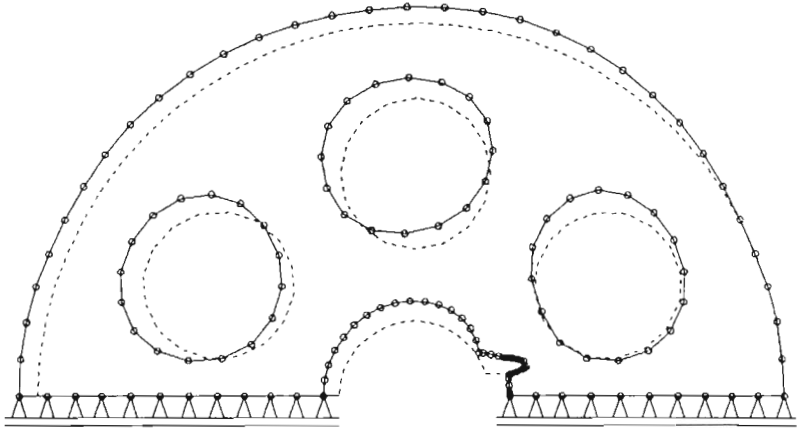


Fig. 8. Initial (dashed line) and deformed shapes (solid line) for the rotating disc with two edge cracks

A rotating disc with seven holes contains two radial edge cracks at the splineway. The dimensions of the disc, expressed in millimeters, are shown in Fig.7. The disc rotates at a constant angular velocity ω and is subjected to centrifugal forces. Because of the disc symmetry only a half of the plate with the proper boundary conditions along the line of symmetry is considered, as shown in Fig.8. The boundary is divided into 66 quadratic elements and 44 domain points are used. In Fig.8 the initial and the deformed shapes of the disc are shown. The DSIFs are normalized with respect to

$$K_0 = \frac{3 - 2\nu}{8(1 - \nu)} \rho \omega^2 R^2 \sqrt{\pi a} \quad (6.2)$$

where R is the disc radius. The normalized stress intensity factors are calculated as $K_I/K_0 = 2.158$ and $K_{II}/K_0 = 0.333$.

6.3. Rectangular bar with an internal square crack

A rectangular bar of width $2b$ and height $2h$ contains the square crack of length $2a$ situated in the centre of the bar, as shown in Fig.9. The ratios are $h/b = 2$ and $a/b = 0.5$. The ends of the bar are subjected to the impact tension σ_0 . The boundary of the body is discretized using 90 quadratic

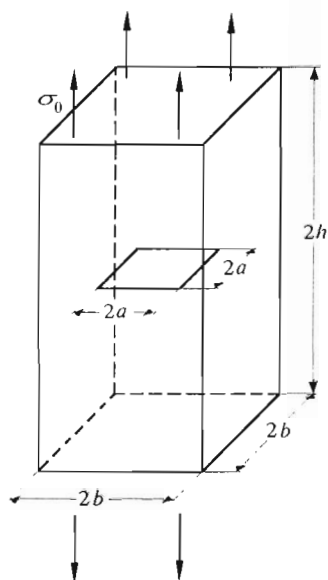


Fig. 9. Rectangular bar with an internal square crack

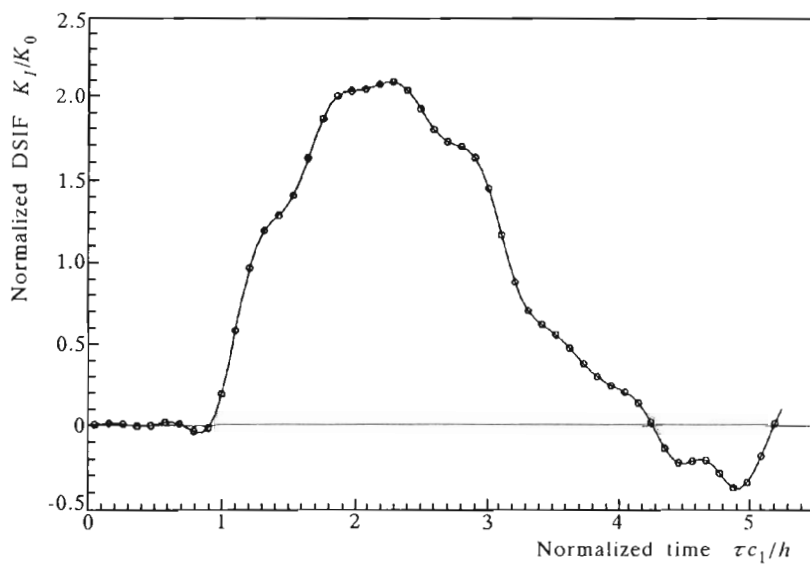


Fig. 10. Normalized DSIF versus normalized time for the rectangular bar with an internal square crack

elements. The normalized DSIFs are plotted as functions of normalized time $\tau c_1/h$ in Fig.10, and as function of normalized frequency $\omega a/c_1$ in Fig.11, where c_1 is the velocity of longitudinal wave.

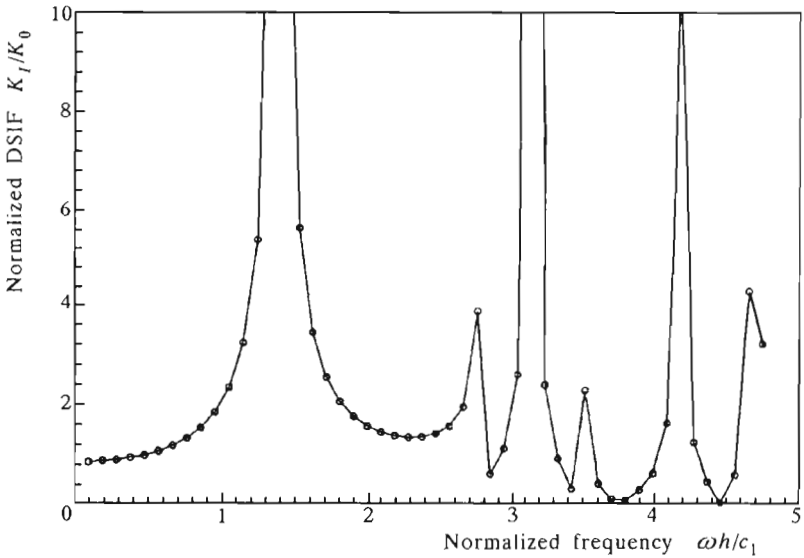


Fig. 11. Normalized DSIF versus normalized forcing frequency for the rectangular bar with an internal square crack

7. Conclusions

The boundary element method is combined with the time-domain method, the integral transform method and the dual reciprocity method. These methods are used to compute the dynamic stress intensity factors for three different problems. Numerical examples demonstrate possible applications of the developed methods.

Acknowledgements

This work was partially supported by the State Committee for Scientific Research under grant No. 8T11F01412.

References

1. ALIABADI M.H., ROOKE D.P., 1991, *Numerical Fracture Mechanics*. Computational Mechanics Publications, Southampton, Kluwer Academic Publishers, Dordrecht
2. BURCZYŃSKI T., 1995, *Metoda elementów brzegowych w mechanice*, Wspomaganie komputerowe CAD-CAM, Wydawnictwa Naukowo-Techniczne, Warszawa (in Polish)
3. CRUSE T.A., 1988, *Boundary Element Analysis in Computational Fracture Mechanics*, Kluwer Academic Publishers, Dordrecht-Boston-London
4. DOMINGUEZ J., 1993, *Boundary Elements in Dynamics*. Computational Mechanics Publications, Southampton
5. FEDELIŃSKI P., 1996, The Fourier Transform Boundary Element Method for Harmonic Vibrations of Cracked Structures, *Scient. Pap. Dept. Engng Mech.*, Gliwice, **2**, 57-62
6. FEDELIŃSKI P., 1997a, Boundary Element Method for Dynamic Analysis of Cracks, *Scient. Pap. Inst. Mat. Sc. Appl. Mech.*, Wrocław, **57**, 139-194 (in Polish)
7. FEDELIŃSKI P., 1997b, Dynamic Crack Growth by Time-Domain Boundary Element Method, in *Proc. XIII Polish Conf. Computer Methods in Mechanics*, Poznań, **1**, 363-370
8. FEDELIŃSKI P., 1997c, The Boundary Element Dynamic Analysis of Structural Elements with Cracks, *Scient. Pap. Dept. Appl. Mech.*, Gliwice, **3**, 37-42
9. FEDELIŃSKI P., 1998a, The Boundary Element Method in Three-Dimensional Dynamic Fracture Mechanics – Part I: Theory, *Scient. Pap. Dept. Appl. Mech.*, Gliwice, **6**, 83-88
10. FEDELIŃSKI P., 1998b, The Boundary Element Method in Three-Dimensional Dynamic Fracture Mechanics – Part II: Examples, *Scient. Pap. Dept. Appl. Mech.*, Gliwice, **6**, 89-94
11. FEDELIŃSKI P., 1998c, The Three-Dimensional Boundary Element Method in Dynamic Analysis of Cracks, *Building Research J.*, (submitted for publication)
12. FEDELIŃSKI P., ALIABADI M.H., ROOKE D.P., 1993a, The Dual Boundary Element Method for Cracked Structures Subjected to Inertial Forces, *BE Abstracts*, **4**, 150-152
13. FEDELIŃSKI P., ALIABADI M.H., ROOKE D.P., 1993b, The Dual Boundary Element Method in Dynamic Fracture Mechanics, *Engng Anal. Bound. Elem.*, **12**, 203-210
14. FEDELIŃSKI P., ALIABADI M.H., ROOKE D.P., 1993c, Dual Boundary Element Method: Inertial Stress Intensity Factors, in *Proc. Boundary Element Technology VIII*, edit. Pina H., Brebbia C.A., Computational Mechanics Publications, Southampton, 267-276
15. FEDELIŃSKI P., ALIABADI M.H., ROOKE D.P., 1994a, The Dual Boundary Element Method: \hat{J} -Integral for Dynamic Stress Intensity Factors, *Int. J. Fracture*, **65**, 369-381

16. FEDELIŃSKI P., ALIABADI M.H., ROOKE D.P., 1994b, The Dual Boundary Element Method for Dynamic Analysis of Cracked Pin-Loaded Lugs, in *Proc. Localized Damage III, Computer Aided Assessment and Control*, edit. Aliabadi M.H. et al., Computational Mechanics Publications, Southampton, 571-578
17. FEDELIŃSKI P., ALIABADI M.H., ROOKE D.P., 1994c, Dynamic Stress Intensity Factors in Mixed-Mode: Time-Domain Formulation, in *Proc. Boundary Elements XVI*, edit. Brebbia C.A., Computational Mechanics Publications, Southampton, 513-520
18. FEDELIŃSKI P., ALIABADI M.H., ROOKE D.P., 1995a, A Single-Region Time-Domain BEM for Dynamic Crack Problems, *Int. J. Solids Struct.*, **32**, 3555-3571
19. FEDELIŃSKI P., ALIABADI M.H., ROOKE D.P., 1995b, Boundary Element Formulations for Dynamic Analysis of Cracked Structures, *Chapter 2, Dynamic Fracture Mechanics*, edit. Aliabadi M.H., Computational Mechanics Publications, Southampton, 61-100
20. FEDELIŃSKI P., ALIABADI M.H., ROOKE D.P., 1996a, The Laplace Transform DBEM Method for Mixed-Mode Dynamic Crack Analysis, *Comp. Struc.*, **59**, 1021-1031
21. FEDELIŃSKI P., ALIABADI M.H., ROOKE D.P., 1996b, Boundary Element Formulations for Dynamic Analysis of Cracked Structures, *Engng Anal. Bound. Elem.*, **17**, 45-56
22. FEDELIŃSKI P., ALIABADI M.H., ROOKE D.P., 1997, The Time-Domain DBEM for Rapidly Growing Cracks, *Int. J. Num. Meth. Engng*, **40**, 1555-1572
23. FREUND L.B., 1990, *Dynamic Fracture Mechanics*, Cambridge University Press, Cambridge
24. MI Y., ALIABADI M.H., 1992, Dual Boundary Element Method for Three-Dimensional Fracture Mechanics Analysis, *Engng Anal. Bound. Elem.*, **10**, 161-171
25. MI Y., ALIABADI M.H., 1994, Three-Dimensional Crack Growth Simulation using BEM, *Comp. Struc.*, **52**, 871-878
26. NEIMITZ A., 1994, *Dynamika wzrostu pęknięć*, Monografie, Studia, Rozprawy, Politechnika Świętokrzyska, Kielce (in Polish)
27. PORTELA A., ALIABADI M.H., ROOKE D.P., 1992, The Dual Boundary Element Method: Effective Implementation for Crack Problems, *Int. J. Num. Meth. Engng*, **33**, 1269-1287
28. PORTELA A., ALIABADI M.H., ROOKE D.P., 1993, Dual Boundary Element Incremental Analysis of Crack Propagation, *Comp. Struc.*, **46**, 237-247
29. WEN, P.H., ALIABADI, M.H., ROOKE, D.P., 1997a, Cracks in Three-Dimensions: a Dynamic Dual Boundary Element Analysis, *Boundary Elements XIX*, edit. Marchetti M., Brebbia C.A., Aliabadi M.H., Computational Mechanics Publications, Southampton, 327-337
30. WEN, P.H., ALIABADI, M.H., ROOKE, D.P., 1997b, A Variational Technique for Three-Dimensional Fracture Mechanics Weight Functions: Dynamic, *Int. J. Num. Meth. Engng*, (submitted for publication)

Metoda elementów brzegowych w analizie dynamicznej pęknięć

Streszczenie

W pracy przedstawiono zastosowanie metody elementów brzegowych w analizie dynamicznej pęknięć. W przyjętym sformułowaniu stosuje się brzegowe równanie całkowe przemieszczeń i sił powierzchniowych dla pęknięcia. Rozwiązania zależne od czasu wyznaczono metodą rozwiązań w dziedzinie czasu, metodą transformacji całkowych i metodą podwójnej zasady wzajemności. Dynamiczne współczynniki intensywności naprężeń obliczono na podstawie przemieszczeń powierzchni pęknięcia i całki \hat{J} niezależnej od drogi całkowania. Przedstawiono nowe przykłady zastosowania metod.

Manuscript received December 12, 1997; accepted for print February 3, 1998